A streamer-like atmospheric pressure plasma jet

Brian L. Sands,[1,a)] Biswa N. Ganguly,[2,b)] and Kunihide Tachibana[3]
[1]*UES, Inc., 2645 5th St., Wright Patterson Air Force Base, Ohio 45433-7251, USA*
[2]*Air Force Research Laboratory, 2645 5th St., Wright Patterson Air Force Base, Ohio 45433-7251, USA*
[3]*Department of Electronic Science and Engineering, Kyoto University, Kyoto-daigaku Katsura, Nishikyo-ku, Kyoto 615-8510, Japan*

(Received 27 February 2008; accepted 25 March 2008; published online 17 April 2008)

The properties of an atmospheric pressure plasma jet (APPJ) are examined in a single-cell dielectric capillary configuration. In contrast to some other flow-driven APPJs, this stable, cold plasma jet is electrically driven, composed of rapidly propagating ionization fronts with speeds of the order of 10^7 cm/s. Using spatially and temporally resolved optical diagnostics, it is demonstrated that the plasma jet is initiated independent of the dielectric barrier discharge inside the capillary. It is also shown that the properties and dynamics of this APPJ are directly analogous to those of positive corona streamer discharges. © *2008 American Institute of Physics*. [DOI: 10.1063/1.2909084]

The atmospheric pressure plasma jet (APPJ) has been studied as a source for generating nonequilibrium atmospheric pressure plasmas for a variety of material processing and biomedical applications. The APPJ source described in this letter is a single-cell dielectric capillary configuration of the form introduced by Teschke *et al.*,[1] which has been subsequently studied in various forms[2,3] and as part of an array device.[4] In contrast to some other APPJ sources, this plasma jet is operated at lower gas flow rates and appears to be electrically driven.[1,2] Time-resolved imagery has shown that the jet is not a continuous volume of plasma, rather it is composed of well defined propagating ionization fronts initially termed as "plasma bullets."[1] These plasma bullets are launched with the rising edge of the voltage cycle and propagate with speeds several orders of magnitude greater than the flow speed.[1,2] Lu and Laroussi[2] proposed a streamer discharge model to explain the properties of these so-called plasma bullets. In this letter, we show that the plasma jet formed outside this dielectric capillary configuration is electrically driven and is independent of the initiation of a dielectric barrier discharge within the capillary. The temporal development and structure of this plasma jet source is similar to that of a self-sustained streamer discharge in free space. This differs from other APPJ sources that exist as a flow-driven effluent sustained from an upstream discharge.

Figure 1 shows our dielectric capillary experimental configuration. A gas mixture of primarily He with a variable Ar concentration was flowed through a cylindrical glass capillary with a 2 mm inside diameter and a 3 mm outside diameter. Copper ring electrodes surrounded the capillary. The anode ring was placed near the end of the capillary and was separated from the cathode ring by ~1 cm. The electrodes were insulated with nylon nuts to prevent arcing outside the capillary. When energized, a capillary dielectric barrier discharge (CDBD) was excited inside this gap with a plasma jet extending beyond the edge of the capillary (cf. Fig. 1). The plasma jet was terminated through a virtual ground plane as no physical electrode was present beyond the capillary. We excited the discharge using a positive-going unipolar voltage pulse with a rise time of 20 ns. Table I lists the ranges of other electrical parameters and ranges for the gas flow rates and mixture ratios that were studied.

Wide bandwidth voltage and current probes were used to monitor the electrical properties. An intensified charge-coupled device (ICCD) camera with a 5 ns gate width was used to monitor the CDBD and plasma jet. Plasma emission was also monitored using two separate fiber-coupled photomultiplier tubes (PMTs). The detector monitoring the CDBD was stationary throughout the experiment, while the plasma jet detector could be translated between 2 and 34 mm from the edge of the capillary. We used the PMTs to measure the relative delay of the emission intensity peaks, for which the measured displacement current peak served as a timing reference. The high degree of shot to shot repeatability, which is a characteristic of this APPJ,[1–3] allowed us to average the PMT signals over 500 shots to more accurately determine the emission delays. Consistent propagation delays related to the PMT response were subtracted from the raw emission delays. The primary error in determining the emission delay was due to the repeatability of the localized emission from the plasma jet and amounted to an error of ± 2 ns. The spatial resolution of the detector was <1 mm. We used 10 nm bandpass filters centered at 340, 390, and 750 nm, respectively, passing 337.1 nm emission from $N_2C\ ^3\Pi_u$-$B\ ^3\Pi_g(0,0)$, 391.4 nm emission from $N_2^+B\ ^2\Sigma_u$-$X\ ^2\Sigma_g(0,0)$, 388.9 nm emission from the He $3\ ^3P$-$2\ ^3S$ metastable transition, and 750.4 nm emission from the Ar $3p^5 4p$-$3p^5 4s$ transition to complement unfiltered broadband measurements.

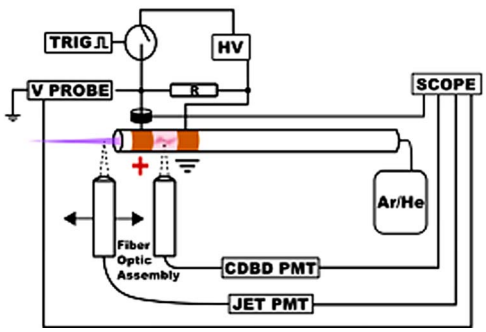

FIG. 1. (Color online) Diagram of the experimental apparatus and the diagnostics used for studying this APPJ source.

a)Electronic mail: brian.sands@wpafb.af.mil.
b)Electronic mail: biswa.ganguly@wpafb.af.mil.

TABLE I. Operating conditions for our dielectric capillary configuration. Conditions used for acquiring the data shown in Figs. 2–4 are listed in parentheses.

Experimental operating conditions	
Applied voltage	10–13(11) kV
Pulse repetition rates	0.6–3.0(1.0) kHz
Total gas flow rates	1.5–9(4.5) slm
Ar/He flow ratios	<1%–25%(5%)

The discharge conditions used to acquire the data in the following figures are listed in parentheses in Table I. Figure 2(a) shows a sequence of unfiltered images of the CDBD and plasma jet taken with the ICCD camera at 20 ns intervals from the onset of emission. The frames from each of the image sequences were integrated over 100 pulses to acquire sufficient signal to noise. The noteworthy feature of Fig. 2(a) is the initiation of the plasma jet *before* the CDBD. This shows that the plasma jet is initiated independent of the discharge inside the capillary and indicates that the jet is a self-sustained discharge that is not directly coupled to the interior discharge. Figure 2(b) illustrates this more precisely with high intensity emission profiles from the 750 nm Ar transition averaged over 500 pulses and acquired with the plasma jet (dashed line) and CDBD (dotted line) PMT detectors. The average total current (solid line) is also shown. The plasma jet detector was focused at ~2 mm beyond the edge of the capillary to ensure that the capillary did not interfere in the measurement. The plasma jet emission at this location consistently led the inner discharge by 5–20 ns over the range of conditions listed in Table I, except for some conditions near the extremes of these ranges where the CDBD and plasma jet were marginally stable. Figure 2(b) represents a typical case with the interior discharge emission lagging by ~10 ns. To confirm the independence of the plasma jet, we

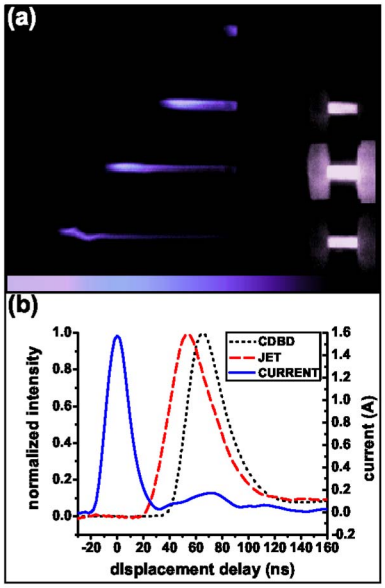

FIG. 2. (Color online) (a) Unfiltered image sequence of the plasma jet and CDBD emission acquired with a 5 ns gated ICCD camera. The frames are at 20 ns intervals from the onset of emission. (b) 750 nm emission profiles acquired with the plasma jet and CDBD PMT detectors and the total current, all averaged over 500 pulses. The data was acquired using a 5% Ar/He gas mixture flowing at 4.5 slm with an 11 kV voltage pulse at a 1 kHz repetition rate.

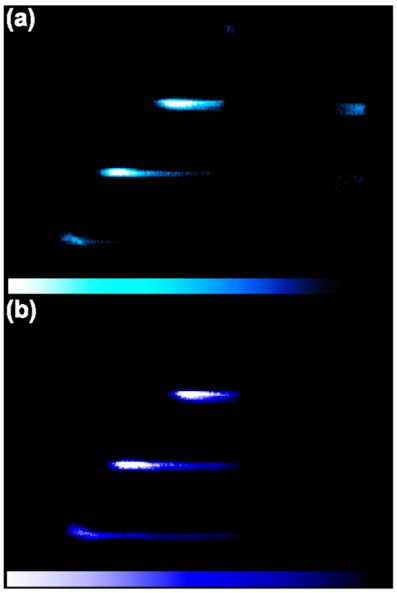

FIG. 3. (Color online) Image sequences acquired with an ICCD camera under the same conditions as Fig. 2. The images show emission through 10 nm bandpass filters centered at (a) 390 and (b) 340 nm.

increased the gap distance by retracting the cathode ring. Under the same discharge conditions, the CDBD emission delay increased from ~10 to >50 ns and became less intense, while the jet emission delay and intensity remained relatively unchanged.

The additional ICCD image sequences in Figs. 3(a) and 3(b) show emission bands centered at 390 and 340 nm, respectively, and illustrate the temporal development and basic structure of the plasma jet. The frames in these sequences were integrated over 600 pulses due to the weaker emission from these bands. More detailed image sequences under the same conditions can be found in Ref. 5. Figure 3(a) tracks the leading ionization front via emission from N_2^+ and excited He and shows it to have a well defined structure. Conversely, emission from the comparatively lower energy N_2 $C\,^3\Pi_u$ state in Fig. 3(b) shows the presence of a weakly ionized plasma channel that can be seen persisting in the wake of the advancing ionization front, establishing current continuity with the anode. These properties are consistent with those of cathode-directed streamers in positive corona discharges.[6,7]

Figure 4 tracks the propagation of the ionization front using the filter centered at 390 nm. The ionization front propagates with a constant velocity over much of the ~3.5 cm length of the jet with an apparent deceleration near the outer edge. The increasing error bars toward the outer edge resulted from a rapidly decreasing signal to noise ratio and temporal fluctuations caused by ambient air currents that tended to broaden the 500 pulse averaged emission profile. The constant propagation velocity was consistent over the range of conditions studied. The propagation speed derived from the linear fit in Fig. 4 was $(5.54 \pm 0.03) \times 10^7$ cm/s. Over the range of parameter space in Table I, the measured speeds varied in a range of $\sim(4-8)10^7$ cm/s and are consistent with previous results.[1,2] The dynamics of the ionization front also closely resemble the dynamics of cathode-directed streamers in a nonuniform field predicted with numerical modeling[7,8] and experimentally observed in positive corona discharges.[9–11] Additionally, Morrow and Lowke[7] showed that a cathode-directed streamer propagating into

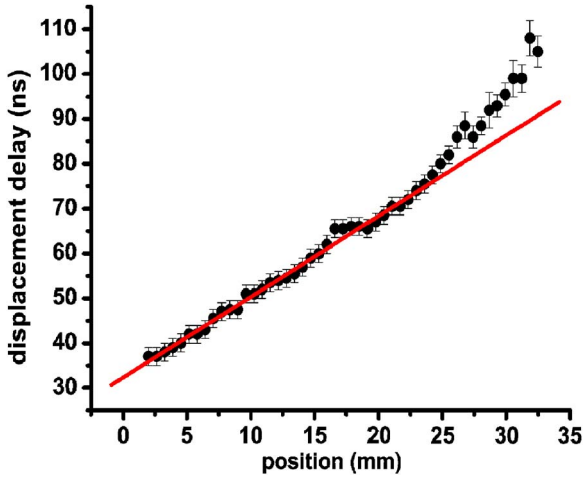

FIG. 4. (Color online) Variation in arrival delay of the plasma jet emission with PMT detector position, measured with respect to the peak of the displacement current for the same operating conditions as Fig. 2 through a 10 nm bandpass filter centered at 390 nm. The propagation speed derived from the linear fit is $(5.54 \pm 0.03) \times 10^7$ cm/s.

free space will terminate once it has propagated to the point where current continuity between itself and the anode can no longer be maintained and the photoionization sustaining its propagation is halted. This resembles our configuration without an external ground plane and it can explain the terminal behavior in Fig. 4. The data shown in Figs. 2–4 depict a very different APPJ source that does not rely on the transport of reactive species from the CDBD in order to form the jet outside the dielectric capillary. Instead, this electrically driven APPJ has properties consistent with a cathode-directed streamer discharge in free space.

There are some notable differences between the streamer-like APPJ source described here and positive corona discharges that are typically used to study cathode-directed streamers. In a typical corona discharge, the electric field diverges outward in a wide angle from the anode and is guided by the presence of a nearby ground plane. This electric field, in turn, guides the streamers, which can develop along several paths with perhaps multiple bifurcations depending on the conditions. Thus, streamer propagation is dependent on the shape of the electric field.[12,13] Streamers developed in pulsed positive corona discharges are typically not very repeatable due to the stochastic nature of their initiation and relatively wide area through which they can propagate. The streamers associated with this configuration are, in contrast, very repeatable and highly directed, consistently tracing the same path. In addition to the presence of a straight flow-gas channel outside the capillary, we also attribute this behavior to the focusing of the electric field along the capillary axis from cylindrically symmetric charge accumulation near the capillary tip during the rising edge of the unipolar voltage pulse, as indicated by the large displacement current in Fig. 2(b). We believe that the short 20 ns rise time of the applied voltage pulse may have led to an increased surface charge accumulation that increased the local E/n and decreased the streamer initiation delay, thus enabling us to observe the initiation of the plasma jet before the interior CDBD. In fact, the plasma jet is particularly sensitive to the capillary tip geometry, which would affect the magnitude and distribution of surface charge. Because it is a challenge to isolate specific streamers in a repeatable fashion in typical corona setups,[14] this APPJ source may be useful as a controlled experiment for the study of streamer discharges.

The results show that the atmospheric pressure plasma jet in this dielectric capillary configuration is initiated *before* the interior CDBD (cf. Fig. 2). This indicates that this plasma jet is a self-sustained discharge and not the flow-driven plasma effluent of the CDBD. We confirmed this by retracting the cathode, which delays the CDBD breakdown, while leaving the plasma jet relatively unchanged. This discharge has streamer-like properties (cf. Figs. 3 and 4), which corroborate the streamer discharge mechanism proposed to explain the rapidly propagating ionization fronts that make up the plasma jet.[2]

We thank David Wisman for assisting in acquiring the ICCD imagery. This work was supported by the U.S. Air Force under Contract No. FA8650-04-D-2404.

[1] M. Teschke, J. Kedzierski, E.. G. Finantu-Dinu, D. Korzec, and J. Engemann, IEEE Trans. Plasma Sci. **33**, 310 (2005).
[2] X. Lu and M. Laroussi, J. Appl. Phys. **100**, 063302 (2006).
[3] J. Walsh, J. Shi, and M. Kong, Appl. Phys. Lett. **88**, 171501 (2006).
[4] O. Sakai, Y. Kishimoto, and K. Tachibana, J. Phys. D **38**, 431 (2005).
[5] B. Sands, B. Ganguly, and K. Tachibana, IEEE Trans. Plasma Sci. (unpublished).
[6] S. Dhali and P. Williams, J. Appl. Phys. **62**, 4696 (1987).
[7] R. Morrow and J. Lowke, J. Phys. D **30**, 614 (1997).
[8] A. Kulikovsky, IEEE Trans. Plasma Sci. **25**, 439 (1997).
[9] W. Yi and P. Williams, J. Phys. D **35**, 205 (2002).
[10] S. Pancheshnyi, M. Nudnova, and A. Starikovskii, Phys. Rev. E **71**, 016407 (2005).
[11] F. Grangé, N. Soulem, J. Loiseau, and N. Spyrou, J. Phys. D **28**, 1619 (1995).
[12] E. van Veldhuizen and W. Rutgers, J. Phys. D **35**, 2169 (2002).
[13] E. van Veldhuizen, A. Baede, D. Hayashi, and W. Rutgers, APP Spring Meeting Bad Honnef, Germany, February 2001, pp. 231–4.
[14] P. Tardiveau, E. Marode, and A. Agneray, J. Phys. D **35**, 2823 (2002).